HgCdTe/CdTe/Si Infrared Photodetectors Grown by MBE for Near-Room Temperature Operation

S. VELICU,[1,5] G. BADANO,[1] Y. SELAMET,[1] C.H. GREIN,[1] J.P. FAURIE,[1] S. SIVANANTHAN,[1] P. BOIERIU,[2] DON RAFOL,[3] and R. ASHOKAN[4]

1.—University of Illinois at Chicago, Microphysics Laboratory, Department of Physics, Chicago, IL 60607. 2.—EPIR Ltd., Bolingbrook, IL 60440. 3.—Jet Propulsion Laboratory, Pasadena, CA 91109. 4.—Smart Pixel Inc., Bolingbrook, IL 60440. 5.—e-mail: silviu@uic.edu

Conventional HgCdTe infrared detectors need significant cooling in order to reduce noise and leakage currents resulting from thermal generation and recombination processes. Although the need for cooling has long been thought to be fundamental and inevitable, it has been recently suggested that Auger recombination and generation rates can be reduced by using the phenomena of exclusion and extraction to produce nonequilibrium carrier distributions. The devices with Auger suppressed operation requires precise control over the composition, and donor and acceptor doping. The successful development of the molecular beam epitaxy (MBE) growth technique for multi-layer HgCdTe makes it possible to grow these device structures. Theoretical calculations suggest that the pπn+ layer sequence is preferable for near-room temperature operation due to longer minority carrier lifetime in lightly doped p-HgCdTe absorber layers. However, because the low doping required for absorption and nonequilibrium operation is easier to achieve in n-type materials, and because Shockley-Read centers should be minimized in order to obtain the benefits of Auger suppression, we have focused on $p^+\nu n$ structures. Planar photodiodes were formed on CdTe/Si (211) composite substrates by As implantation followed by a three step annealing sequence. Three inch diameter Si substrates were employed since they are of high quality, low cost, and available in large areas. Due to this development, large area focal plane arrays (FPAs) operated at room temperature are possible in the near future. The structures were characterized by FTIR, x-ray diffraction, temperature dependent Hall measurements, minority carrier lifetimes by photoconductive decay, and in-situ ellipsometry. To study the relative influence of bulk and surface effects, devices with active areas from 1.6×10^{-5} cm^2 to 10^{-3} cm^2 were fabricated. The smaller area devices show better performance in terms of reverse bias characteristics indicating that the bulk quality could be further improved. At 80 K, the zero bias leakage current for a 40 μm × 40 μm diode with 3.2 μm cutoff wavelength is 1 pA, the R_0A product is 1.1×10^4 Ω-cm^2 and the breakdown voltage is in excess of 500 mV. The device shows a responsivity of 1.3×10^7 V/W and a 80 K detectivity of 1.9×10^{11} cm-Hz$^{1/2}$/W. At 200 K, the zero bias leakage current is 5 nA and the R_0A product 2.03 Ω-cm^2, while the breakdown voltage decreases to 40 mV.

Key words: HgCdTe, infrared detectors, MBE

INTRODUCTION

Present day near-room-temperature infrared photon detectors display sub-background limited performance (BLIP). Background limited performance and high sensitivities are required for many strategic, space, and spectroscopic applications. It would be highly desirable to preserve the near-BLIP performance at 77 K of HgCdTe-based infrared (IR) detectors but increase the operating temperature. The main obstacle in achieving this goal is the large level

(Received November 25, 2000; accepted December 19, 2000)

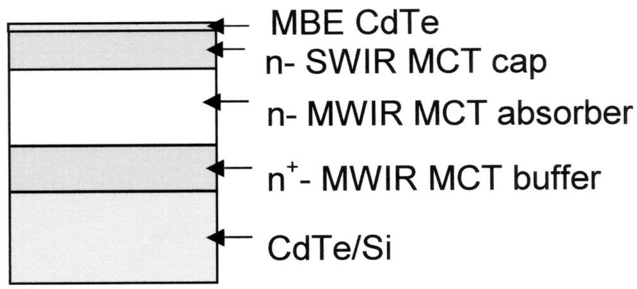

Fig. 1. MBE grown HgCdTe nνn+ heterostructure.

of noise due to Auger generation and recombination near room temperature. Ashley and Elliott[1] proposed the suppression of the Auger process by reducing the electron and hole concentrations below their equilibrium values. Two configurations—pνn+ and nπp+—are possible to achieve such nonequilibrium devices. It has long been realized[2] that the lifetime in Auger-dominated HgCdTe devices is larger in p-type material than in n-type material. Hence, the pπn+ structure would be preferable for the near-room temperature operation of non-equilibrium detectors from a thermal generation rate point of view. The pπn+ structures have been grown by metalorganic vapor phase epitaxy (MOVPE) and the Auger generation in the π layer was found to be the limiting mechanism.[3] In a recent study, Elliott et al.[4] have shown that the doping required for background limited behavior in the mid-wavelength infrared (MWIR) spectral range in a detector with a 2π field of view is in mid 10^{14} cm^{-3} range, difficult to achieve with the today's MOVPE technology. The molecular beam epitaxy (MBE) growth technique offers the capability for n-type doping in the low 10^{14} cm^{-3} range. Also, the quality of indium doped n-HgCdTe layers is well known to be better than As-doped p-HgCdTe layers mainly because Shockley-Read centers degrade p-type material much more than n-type material. This leads to increased mobilities and increased minority carrier lifetimes for n-type material. To realize Auger-suppressed devices, an epitaxial process with independent control of composition and doping is critical. The use of Si, a high quality and cost-effective substrate that is available in large areas, creates the possibility for large format focal plane arrays (FPAs) operated at room temperature in the near future. Preliminary results on the application of the MBE technique to grow HgCdTe device structures on Si substrates, particularly to satisfy the low donor concentration requirements, and the potential for near-room temperature operation of HgCdTe-based devices are discussed in this paper.

DEVICE STRUCTURE AND MODELING

Based on the above facts, we focused on p+νn device structures. A schematic of such a non-equilibrium photodiode is shown in Fig. 1. This device structure involves both exclusion at the nν contact and extraction at the νp+ contact. It offers an improvement over the conventional two-layer type of junction even in an equilibrium mode of operation because the volume from which thermally generated carriers are collected on the low-doped side of the junction is limited by a low surface recombination velocity.

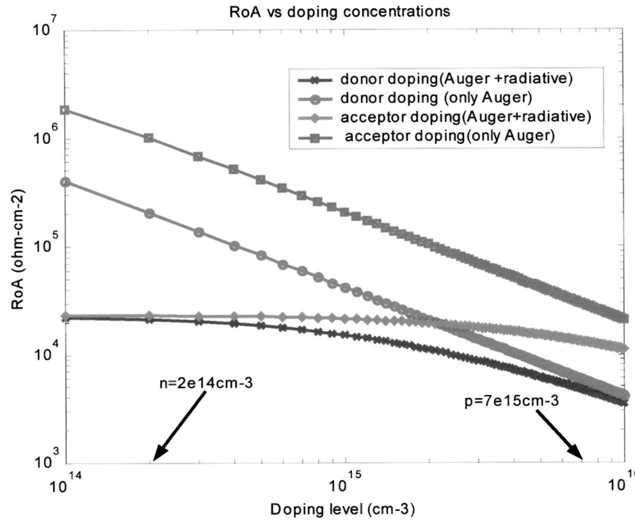

Fig. 2. Theoretical R_0A product with and without radiative recombination mechanism included.

We performed preliminary calculations based on the model developed by Tennant and Cabelli.[5] The model assumes that the dominant current is diffusion from the absorption region. The influence of the interfaces, of the depletion region, and of the heavily doped side of the junction are neglected. Both radiative and Auger mechanisms are used for the computation of the minority carrier lifetimes. However, according to Humphrey's[6] theory, radiative recombination does not limit the performance of the diode due to the reabsorption of the photons generated by recombination within the detector. Because the reabsorption time is very small (<1 ps), the associated process is found to be noiseless. We calculate the R_0A product according to both Humphrey's and van Roesbroeck's[7] theories. We also slightly modified the Tennant model to allow for the computation of the R_0A product in n^+p diodes and to compare n^+p and p^+n structures. The ratio of the intrinsic Auger 7 to Auger 1 lifetime is taken from Ref. 2:

$$\gamma = \frac{6(1-5E_g/4kT)}{1-3E_g/2kT} \tag{1}$$

where E_g is the bandgap of the absorber layer, k is the Boltzman's constant, and T is the temperature.

We computed the dependence of the R_0A product on the doping concentration in both n- and p-type absorber layers. The results are presented in Fig. 2 with and without radiative recombination mechanisms included. We assumed total carrier extraction so that the Auger and radiative rates are determined only by the extrinsic doping. It can be seen that a low 10^{14} cm^{-3} donor doping gives a better R_0A product than a high 10^{15} acceptor doping. As we will show later, mid and

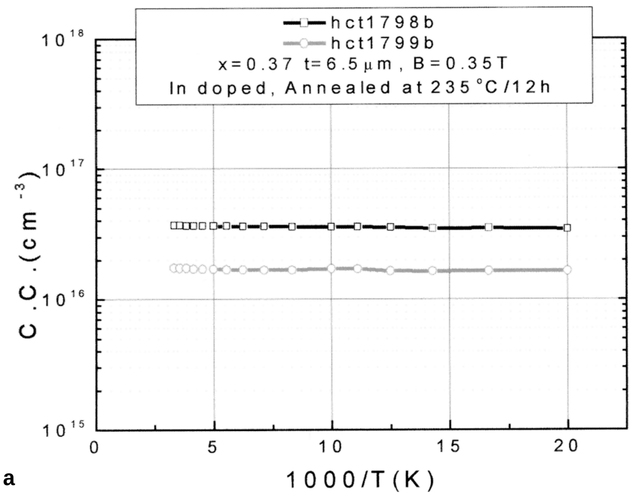

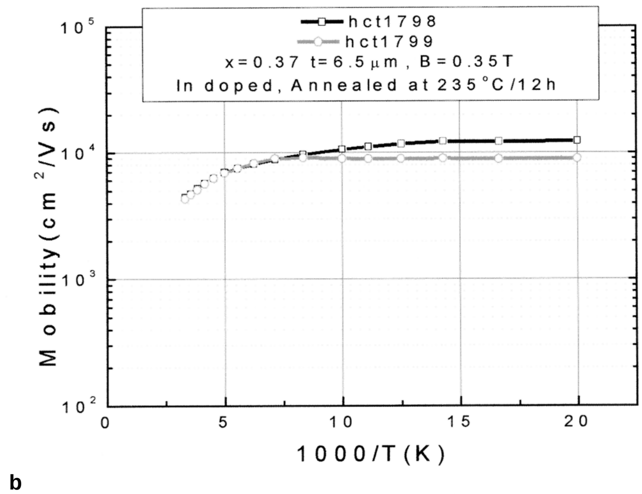

Fig. 3. Temperature dependence of the (a) carrier concentration and (b) mobility after annealing for the first batch of MWIR samples.

even low 10^{14} cm^{-3} donor levels are experimentally achievable using the MBE technique. For vacancy or extrinsic doped HgCdTe, the acceptor level in a p-type absorber is difficult to control at these low levels. So, even if theoretically higher lifetimes are expected because γ is computed to be greater than unity in lightly doped p-type HgCdTe, we believe that a practical way to achieve high temperature performance is to use an n-type absorber layer. At near-room temperature, the absorber is intrinsic and the minority carrier extraction occurs at the reverse biased νp^+ junction. The minority carrier hole will not be injected into the absorber layer when the νp^+ junction is reverse biased because the p^+ layer is of a wider band gap. As a result, the net hole concentration in the absorber layer will fall by orders of magnitude. To maintain charge neutrality, the majority carrier concentration decreases to the extrinsic doping level. The isotype junction, nν, forms an excluding hi-lo type of contact to the central absorber region, thus preventing the injection of carriers to replace those extracted at the diode junction. The n contact is a low recombination velocity interface and does not contribute to the dark current due to both band bending and to band filling to such a degree that Auger 1 generation is quenched in that volume. It is important to note that the electric fields are sufficiently low to avoid carrier heating since the extraction process is principally a diffusion process. The reverse bias should be chosen to exceed the critical field necessary for the extraction process, but kept below a certain level to avoid the carrier heating. Calculations by Ashley and Elliott indicate that the required exclusion field can be achieved in the MWIR HgCdTe diodes over a wide range of doping levels without exceeding the estimated field for carrier heating.

EXPERIMENT

The structures, as shown in Fig. 1, were grown on CdTe/Si(211) substrates by MBE. The MBE growth chamber is equipped with an in-situ reflection high-energy electron diffraction (RHEED) gun and an ellipsometer to achieve real-time monitoring of the crystalline structure and the composition. CdTe(211)/Si substrates, with x-ray rocking curve full width at half maximum (FWHM) lower than 100 arcsec and etch pit densities below 10^5 cm^{-2}, were used for the HgCdTe growth.

The targeted structure for this growth consists of three HgCdTe layers capped with a CdTe layer, as indicated in Fig. 1. The first HgCdTe layer from the top is short wave infrared (SWIR), n-type doped with indium in-situ during the growth. The second layer is a ν-type doped MWIR absorber layer, with targeted CdTe mole fraction of about 0.3 and carrier concentration below 2×10^{15} cm^{-3}. The third layer is a heavily doped MWIR layer. The planar p-n junction is formed by selective ion implantation with 75 As^{++}. A three-step post-implant anneal places the electrical junction on the narrow gap side of the junction and also reduces the residual defects in the ν-MCT layer. The samples were characterized by Fourier transform infrared spectroscopy (FTIR), x-ray rocking curves, Hall and lifetime measurements to determine the crystalline, optical and electrical properties.

FTIR measurements have been performed to determine the thickness of the layers and the composition of the absorber. The data were fit to a multi-layer structure model[8] that allows the determination of the thickness of each layer. The data for four such samples are presented in Table I. The x-ray rocking curve data were fitted to obtain the FWHM of the peaks. From the fitting, the FWHM obtained was 194 arcsec for CdTe, and 106 for HgCdTe. The latter value is close to the FWHM of the substrate, and is reasonably good for HgCdTe layers grown on CdTe/Si substrates indicating good structural quality of the material.

Temperature dependent Hall effect measurements were carried out after etching away the top CdTe and wider bandgap HgCdTe layers and annealing at 235°C for 12 hours for Hg vacancy filling. The measured carrier concentration at 77 K in the first batch

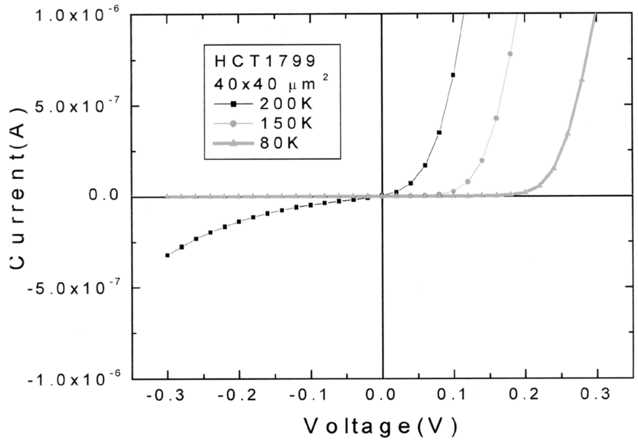

Fig. 4. I-V characteristics of a 40 × 40 μm^2 test diode (λ_c = 3.2 μm) at three different temperatures.

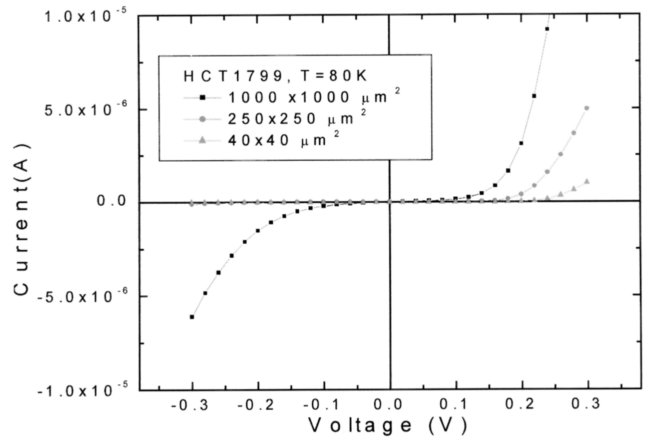

Fig. 5. I-V characteristics of three diodes (λ_c = 3.2 μm) of different area at 80 K.

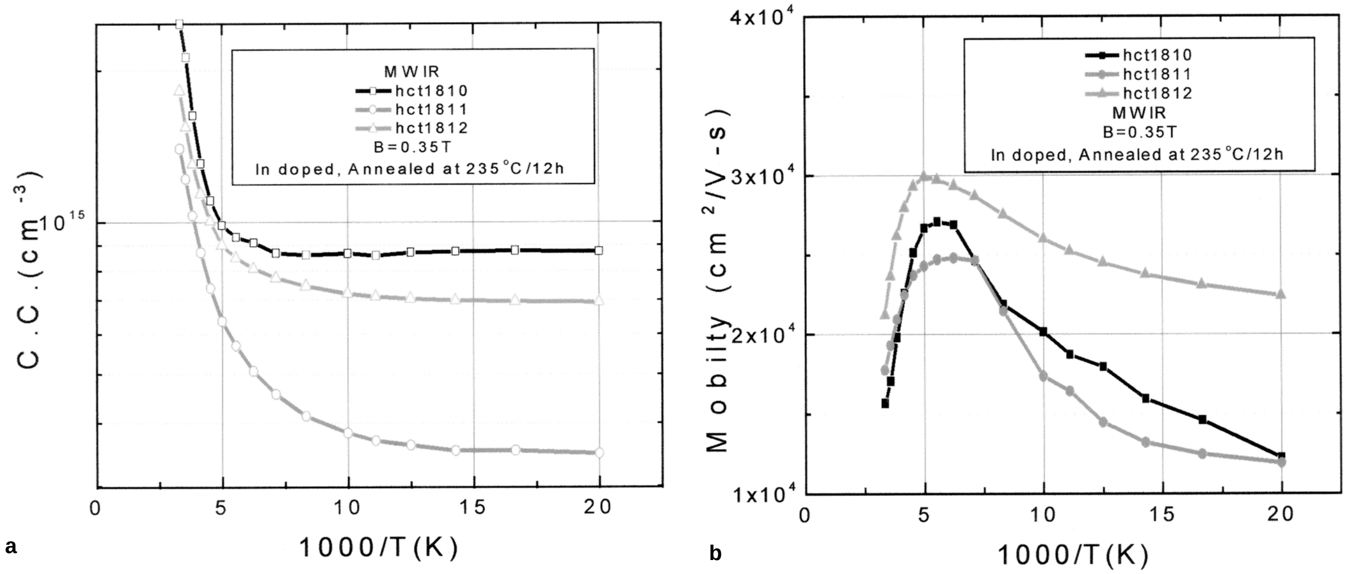

Fig. 6. Temperature dependence of the (a) carrier concentration and (b) mobility after annealing for an optimized batch of MWIR samples.

(HCT1798, HCT1799) was in the 1–4 × 10^{16} range, while the mobility was around 10000 cm^2/V-sec, reflecting the fact that, at this depth, an average between the mobility of the lightly doped and the heavily doped deeper layers is measured, as shown in Fig. 3. Because of the high extrinsic dopant concentration in the absorption layer, no carrier extraction was observed in the processed devices. However, as we mentioned before, a reasonably high R_0A product is obtained because of the low recombination velocity of the $n^+\nu$ contact. Also, the measured detectivity (discussed later) indicates the feasibility of HgCdTe based infrared detectors for near room temperature operation.

AutoCAD software was used to prepare the layout of the masks needed for the fabrication of these devices. An automatic pattern generator was used for the fabrication of high quality chrome/iron oxide masks. The devices were fabricated using a MJB-3 contact mask aligner, indium, titanium, gold metallization systems, and other common device fabrication facilities. In the first lithography step, windows for As implantation are opened. Thick photoresist was used as the mask layer. After ion implantation (350 KeV energy, 10^{14} cm^{-2} dose), the samples were subjected to a three-step temperature anneal under mercury saturated conditions for the activation of dopants and the removal of Hg vacancies. The P-HgCdTe contacts using a gold chloride solution and the n-type contacts using In deposition were made. After that, Ti/Au contact/bonding pads are deposited. The distance between different diodes is larger than the minority carrier diffusion length so we can assume independent operation.

RESULTS AND DISCUSSION

I-V characteristics were measured in a low temperature probe station with 300 K background. To avoid any damage during testing, the pads were placed away from the active area. The temperature dependence of the I-V curves of these devices was studied and the results are presented in Fig. 4 at

Table I. Thickness and Composition of the Layers from FTIR Data Fitting

	HCT1799		HCT1810		HCT1811		HCT1812	
	x*	t**	x*	t**	x*	t**	x*	t**
SWIR cap layer	0.45	0.5	0.42	0.8	0.49	0.47	0.39	0.74
MWIR absorber layer	0.37	5	0.33	9	0.39	6.10	0.33	9.75
MWIR buffer Layer	0.37	2	0.33	2	0.39	2.30	0.33	3.75

*—Cd comp; **—thickness (μm)

Table II. Hall Concentration and Minority Carrier Lifetime at 80 K

Sample	Carrier Concentration (cm^{-3})	Mobility (cm^{-2}/V-sec)	Measured Lifetime (μs)	Theoretical Lifetime (Rad+Auger)
Hct1810	9×10^{14}	17900	1.45	5.4
Hct1811	2.5×10^{14}	14290	2.45	17.5
Hct1812	6.9×10^{14}	24300	2.50	7.3

80 K, 150 K, and 200 K for a 40×40 μm^2 device. The forward turn-on voltage decreases with increasing temperature as expected from the band gap dependence on temperature and the breakdown voltage decreases to approximately 400 mV at 200K, in comparison with >500 mV at 80 K. For the 40×40 μm diodes the zero bias leakage current is about 1 pA and the R_0A is 1.1×10^4 ohm-cm^2 at 80 K. Tunneling currents become dominant at voltages larger than 500 mV. We show in Fig. 5 the I-V characteristics for diodes of different area. It can be seen that the device quality improves when the diode area is decreased. As we have shown in a previous study,[9] this is an indication that the bulk has an important contribution in degrading diode performance. Large area diodes have more probability to circumvent killer defects and their performance reflects the quality of the bulk material. The surface contribution to the dark current is expected to further reduce by removing the damaged CdTe cap layer after post-implant annealing and re-passivating the surface. In this batch of devices we have used the original grown CdTe layer for passivation. Substantial damage occurs in this layer due to the high energy implantation and annealing processes. The R_0A product is consequently lower than the best achieved in these type of devices, resulting in lower detectivities than expected theoretically. Responsivity measurements were carried out at 80 K and 300 K on the 40×40 μm^2 diode at the background temperature of 300 K using a blackbody at 500 K, an aperture size of 0.2 inch, distance between the blackbody and detector of 5 inch, and the chopper frequency at 1000 Hz. The measured responsivity was 1.3×10^7 V/W and hence the detectivity was 1.9×10^{11} cm-Hz$^{1/2}$/W at 80 K and 1×10^{10} cm-Hz$^{1/2}$/W at 300 K. The theoretically expected values[10] are in the range of high 10^{11} and mid 10^{10} cm-Hz$^{1/2}$/W at 80 K and 300 K, respectively. The noise measurement was performed with zero bias voltage and 10 Hz bandwidth. The measured knee frequency, f_k, in this device is 100 Hz at 80 K, a consequence of the lower cut-off wavelength and fairly good electrical properties. For a comparative device[11] at 80 K with I_s = 14 nA and R_0A = 10 Ω-cm^2, the f_k is 4 Hz and increases to 6 MHz for uncooled operation. For this reason, even though the detectivity (3×10^9 Jones) is superior to pyroelectric devices, these devices could not be used for imaging applications. The knee frequency depends mainly on leakage current density and passivation conditions. To reduce the f_k and 1/f noise further, improvements in both bulk and surface properties are needed.

In the subsequent growth, doping level in the low 10^{14} cm^{-3} and mobility in the mid 10^4 cm^2/V-sec were obtained, as shown in the Fig. 6, following the same procedure described previously. This indicates a continuous improvement in the growth conditions. The mobility values are in the same range as those measured on samples grown on CdZnTe substrate. The composition and thickness obtained from FTIR measurements for three samples grown under the optimized condition (HCT1810, HCT1811, and HCT1812) are presented in Table I. Minority carrier lifetime measurements were also performed on these samples using the photoconductive decay technique at 80K, using a pulsed GaAs diode laser with a 90 ns pulse width and a fall time of 70 ns. Close to theoretical Auger and radiative lifetimes were obtained as shown in Table II, indicating low density of Shockley-Read centers. However, the relative independence of doping suggests that both band-to-band and some form of Shockley-Read mechanism limit these lifetimes. A summary of the Hall and lifetime data is presented in the Table II. Exclusion and extraction are expected to occur in devices fabricated from these layers.

CONCLUSIONS

Triple layer pvn$^+$ devices were grown by MBE on Si substrates. Electrical and optical characterization of these devices demonstrates that HgCdTe has the potential for higher temperature operation. The measured responsivity 1.3×10^7 V/W and the calculated detectivity 1.9×10^{11} cm-Hz$^{1/2}$/W of a 40×40 μm^2 diode at 80 K are promising results. A room temperature detectivity of 10^{10} cm-Hz$^{1/2}$/W is the best reported result for a HgCdTe/Si pvn$^+$ structure, to the best of our knowledge. A low donor doping concentration in the 10^{14} cm^{-3} range for the HgCdTe absorber layer by MBE is demonstrated for the first time and creates the possibility for exclusion-extraction devices in the near future.

REFERENCES

1. T. Ashley, C.T. Elliott, and A.T. Harker, *Infrared Phys.* 26, 303 (1986).
2. T.N. Casselman, *J. Appl. Phys.* 52, 848 (1981).
3. C.T. Elliott, N.T. Gordon, R.S. Hall, T.J. Phillips, and A.M. White, *J. Electron. Mater.* 38, 1139 (1996).
4. C.T. Elliott, N.T. Gordon, and A.M. White, *Appl. Phys. Lett.* 78, 2881 (1999).
5. W.E. Tennant and C. Cabelli, *Mater. Res. Soc. Symp. Proc.* 484, 221 (1998).
6. R.G. Humphreys, *Infrared Phys.* 23, 171 (1983).
7. W. van Roosbroeck and W. Shockley, *Phys. Rev.* 94, 1558 (1954).
8. M. Daraselia, C.H. Grein, S. Rujirawat, B. Yang, S. Sivananthan, F. Aqariden, and H.D. Shih, *J. Electron. Mater.* 28, 743 (1999).
9. R. Ashokan, N.K. Dhar, B. Yang, A. Akhiyat, T.S. Lee, S. Yusuf, and S. Sivananthan, *J. Electron. Mater.* 29, 636 (2000).
10. T.S. Lee, R. Ashokan, C.H. Grein, S.S. Yoo, and S. Sivanathan, *Proc. of SPIE* 374,4028 (2000).
11. C.L. Jones, N.E. Metcalfe, A. Best, R. Catchpole, C.D. Maxey, N.T. Gordon, R.S. Hall, T. Colin, and T. Skauli, *J. Electron. Mater.* 27, 733 (1998).